Published in final edited form as:
J Immunol. 2008 November 15; 181(10): 7176–7185.

TLR/MyD88 and LXRα Signaling Pathways Reciprocally Control *Chlamydia Pneumoniae*-Induced Acceleration of Atherosclerosis

Yoshikazu Naiki[1,7], **Rosalinda Sorrentino**[1], **Michelle H. Wong**[1], **Kathrin S. Michelsen**[1], **Kenichi Shimada**[1], **Shuang Chen**[1], **Atilla Yilmaz**[2], **Anatoly Slepenkin**[3], **Nicolas W. J. Schröder**[1], **Timothy R. Crother**[1], **Yonca Bulut**[1], **Terence M. Doherty**[1], **Michelle Bradley**[4], **Zory Shaposhnik**[5], **Ellena M. Peterson**[3], **Peter Tontonoz**[4], **Prediman K. Shah**[6], and **Moshe Arditi**[1]

1 *Divisions of Pediatric Infectious Diseases Cedars–Sinai Medical Center and David Geffen School of Medicine, University of California, Los Angeles, CA 90048*

2 *Medical Clinic II, University of Erlangen-Nuremburg, 91054 Erlangen, Germany*

3 *Department of Pathology, University of California Irvine, Irvine, California 92697*

4 *Department of Molecular Biology Institute, University of California, Los Angeles, CA 90095*

5 *Division of Cardiology, University of California, Los Angeles, CA, 90095*

6 *Division of Cardiology and Oppenheimer Atherosclerosis Research Center, Cedars Sinai Medical Center and the University of California, Los Angeles, CA 90048*

7 *Department of Microbiology and Immunology, Aichi Medical University, Nagakute, Aichi 480-1195, Japan*

Abstract

Experimental and clinical studies link *Chlamydia pneumoniae* infection to atherogenesis and athero-thrombotic events, but the underlying mechanisms are unclear. We tested the hypothesis that *C. pneumoniae*-induced acceleration of atherosclerosis in ApoE$^{-/-}$ mice is reciprocally modulated by activation of TLR-mediated innate immune or LXRα signaling pathways. We infected ApoE$^{-/-}$ mice and ApoE$^{-/-}$ mice that also lacked TLR2 or TLR4 or MyD88 or LXRα intranasally with *C. pneumoniae* followed by high-fat diet feeding for 4 months. Mock infected littermates served as controls. Atherosclerosis was assessed in aortic sinuses and in *en face* preparation of whole aorta. The numbers of activated dendritic cells (DCs) within plaques, and serum levels of cholesterol and proinflammatory cytokines were also measured. *C. pneumoniae* infection markedly accelerated atherosclerosis in ApoE deficient mice that was associated with increased numbers of activated DCs in aortic sinus plaques and higher circulating levels of MCP-1, IL-12p40, IL-6 and TNF-α. In contrast, *C. pneumoniae* infection had only a minimal effect on atherosclerosis, accumulation of activated DCs in the sinus plaques, or circulating cytokine increases in ApoE$^{-/-}$ mice that were also deficient in either TLR2, TLR4, or MyD88. However, *C. pneumoniae*-induced acceleration of atherosclerosis in ApoE$^{-/-}$ mice was further enhanced in ApoE$^{-/-}$/LXRα$^{-/-}$ double knockout mice, and was accompanied by higher serum levels of IL-6 and TNF-α. We conclude that *C. pneumoniae*-infection accelerates atherosclerosis in hypercholesterolemic mice predominantly through a TLR/MyD88-dependent mechanism, and that LXRα appears to reciprocally modulate and reduce the pro-atherogenic effects of *C. pneumoniae* infection.

Corresponding Author: Moshe Arditi, MD. Cedars Sinai Medical Center, Division of Pediatric Infectious Diseases and Immunology, 8700 Beverly Blvd. Rm 4221. Los Angeles, California, 90048, USA. Phone: (310) 423-4471; Fax: (310) 423 8284; Email: E-mail: moshe.arditi@cshs.org.

INTRODUCTION

Experimental and clinical studies demonstrate a link between *Chlamydia pneumoniae* infection and increased atherosclerosis and atherothrombotic events (1). *C. pneumoniae* has been isolated from the coronary arteries of patients with acute coronary syndrome (2), and from human aorta (3), carotid arteries (4), and peripheral arteries (5). Infection of cholesterol-fed C57BL/6 mice with *C. pneumoniae* produces aortic sinus lesions that are twice as large as those in uninfected control mice (1,6). Most reports using murine models of atherosclerosis also indicate that *C. pneumoniae* infection exacerbates atherosclerosis compared to uninfected mice (7–10), although some studies have failed to find such a link (11,12).

The precise mechanism(s) by which *C. pneumoniae* infection might accelerate atherosclerosis are unclear, but there are suggestions that mononuclear phagocytes and innate immune signaling may be involved. *C. pneumoniae* can infect and survive in circulating monocytes and tissue macrophages (13,14), and can migrate from the lung to developing plaques via circulating monocytes and lymphocytes. Experimental studies have previously demonstrated that activation of innate immune signaling emanating from Toll-like receptors (TLRs) increases atherosclerosis in mice (15–18) and that *C. pneumoniae* can activate innate immunity via TLR-dependent signaling (19). Since mononuclear phagocytes express TLRs, it is conceivable that the ability of *C. pneumoniae* to promote atherogenesis could at least partly be explained by TLR-dependent effects of the pathogen (or molecules derived from the pathogen) on macrophages.

Macrophages take up necrotic cellular debris that accumulate in lesions, lose migratory ability, and eventually can become transformed into plaque foam cells that can promote further plaque development and focal inflammation (20,21). However, macrophages are also intimately involved in cholesterol homeostasis. Macrophage lipid uptake is counterbalanced by the activation of liver X receptors (LXR), which exist in two isoforms, LXRα and β. These nuclear receptors importantly regulate cholesterol absorption, transport and efflux (22,23). LXRs are activated by oxysterols and products of cholesterol, but they exert anti-inflammatory effects in macrophages by modulating the activation of NF-κB (24). Furthermore, LXR-dependent and TLR-dependent signaling and/or downstream effects appear to reciprocally modulate one another (23,25).

Collectively, these data led us to hypothesize that the effects of *C. pneumoniae* on atherosclerosis might be reciprocally modulated by activation of innate immunity through TLR/MyD88-dependent and LXRα–dependent signaling pathways. We report that infection with *C. pneumoniae* in hypercholesterolemic ApoE$^{-/-}$ mice increases atherosclerosis that is significantly inhibited in ApoE$^{-/-}$ mice lacking TLR2, TLR4, or MyD88, but in contrast, is enhanced in ApoE/LXRα double knockout mice. Thus, in the context of hypercholesterolemia, *C. pneumoniae* infection directly promotes atherosclerotic plaque development via the TLR/MyD88-dependent signaling pathways, but this is countered by LXRα activation. These results provide novel insight into how *C. pneumoniae* infection impacts atherogenesis, and suggest that therapeutic targeting of TLR2, TLR4, and LXRα signaling pathways might prove beneficial in treating atherosclerosis.

MATERIALS AND METHODS

Generation of Double Knockout Mice

MyD88$^{-/-}$, TLR2$^{-/-}$, TLR4$^{-/-}$, and LXRα$^{-/-}$ mice were crossed with ApoE$^{-/-}$ C57BL/6 mice as we previously described (16). Heterozygous mice were intercrossed to generate homozygous ApoE$^{-/-}$ mice bearing combinations of MyD88$^{+/+}$, $^{+/-}$, $^{-/-}$, TLR4$^{+/+}$, $^{+/-}$, $^{-/-}$, and TLR2$^{+/+}$, $^{+/-}$, and $^{-/-}$ mice as we previously described (16). This process resulted in a backcross

for a total of eight generations onto the C57BL/6 background. ApoE$^{-/-}$/TLR2$^{+/+}$, ApoE$^{-/-}$/TLR4$^{+/+}$, ApoE$^{-/-}$/MyD88$^{+/+}$, and ApoE$^{-/-}$/LXRα $^{+/+}$ were used as littermate controls. Mice were fed with a high fat diet (HFD) containing 0.15% cholesterol (Harlan Teklad, Madison, WI) starting at 8 weeks of age prior to infection and continuing till sacrifice. Mice were maintained under specific pathogen-free conditions, and were used at 8 weeks of age. Male and female ApoE$^{-/-}$ and double knockout mice were used, but the vast majority of the animals in each group were male (over 80% in each group investigated). All experiments were approved by the Cedars–Sinai Medical Center Institutional Animal Care and Use Committee and performed according to institutional guidelines.

C. pneumoniae Infection

C. pneumoniae strain CM-1 (ATCC, Manassas, VA) was propagated in Hep-2 cells as previously described. Hep-2 cells and the *C. pneumoniae stocks* were determined to be free of Mycoplasma contamination by PCR. Mice were anesthetized with isofluorane prior to intranasal (i.n.) application of 5×10^4 IFU/mouse of *C. pneumoniae* suspended in sucrose-phosphate-glutamate buffer (40 μl per nostril). The intranasal administration of the buffer alone was performed as a negative control (mock infection, data not shown). Mice were inoculated a total of three times one week apart, and after the last inoculation, a high fat diet was initiated and continued for 4 months, at which point mice were sacrificed and dependent variables measured (Fig 1A).

Assessment of Atherosclerotic Lesions in the Aorta and Aortic Sinus

Mice were anesthetized with isofluorane before the aorta and the heart were excised. Aortas were excised, from the aortic arch to the iliac bifurcation. Adherent (advential) connective fat was removed, and specimens were then fixed in Histo-CHOICE (Amrecso, Solon, OH). Whole aortas were opened longitudinally and mounted *en face*, then stained for lipids with Oil red O. Hearts were embedded in OCT compound (Tissue Tek, Sakura, Torrance, CA), and cross sections of the aortic sinus were stained with Oil red O. Lesions areas were quantified with Image-Pro Plus (Media Cybernetics, Silver Spring, MD). Image analysis was performed by a trained observer blinded to the genotypes of mice as previously described (16). The lesion area and lipid-stained areas in the aortic sinus and the aorta were measured. The lesion size in the aortic sinus was expressed as "Aortic Sinus Lesion Area ($\times 10^5$ μm^2/section) and the plaque composition in the aortic sinus was expressed as "Lipid content Aortic Sinus" (% plaque area staining with lipid). Five serial sections per animal were analyzed with the resulting data averaged and presented as average aortic sinus lesion area. The lesion area in the aorta en face preparations was expressed as "Aortic Lesion Coverage" (% total aortic surface staining with lipid) as previously reported (16).

Immunohistochemical Staining and Quantification of Dendritic Cells in the Aortic Sinus

Frozen heart sections (aortic sinuses) were analyzed for infiltration of activated dendritic cells (DCs) using rat anti-mouse MIDC-8 Ab (Serotec) using the CSA-kit from DakoCytomation) as we described previously (26). Secondary biotinylated Ab was used followed by streptavidin-biotin-peroxidase complex. An isotype control (IgG2a; Serotec) was used to demonstrate specificity of staining. The rat mAb MIDC-8, which binds a still unidentified antigen within intracellular granules of mature, myeloid DCs (27,28) has been used in multiple studies as a specific marker of mature (activated) myeloid DCs (27–29) including in murine atherosclerosis in ApoE-null mice (30). Pictures of the aortic sinuses were taken (330x) with a CCD camera (Nikon). The stained DCs (MIDC8+) were determined in three representative aortic sinus regions (0.10 μm^2) as described (26). The number of activated DCs was quantified using Image-Pro Plus software (Media Cybernetics, Silver Spring, MD).

Lipid Profiles

Total cholesterol concentrations were determined in duplicate by using a colorimetric assay (infinity cholesterol reagent, Sigma Diagnostics, St. Louis). Triglyceride concentrations were determined by using the L-type triglyceride H assay according to the manufacturer's instructions (Wako Chemicals USA, Richmond, VA). These assays were performed on serum obtained from blood withdrawn at the time of sacrifice from mice that had undergone an overnight fast.

Serum Levels of Cytokines and Chemokines

Serum concentrations of TNFα, IL-6, IL12p40 and MCP-1 (BD Biosciences and R&D for MCP-1) were detected by means of ELISA according to the manufacturer's instructions.

Assessment of Foam Cells

Peritoneal macrophages were isolated from C57BL/6 wild-type mice after the instillation of PBS buffer with 2mM of EDTA (Sigma, USA). Cells were plated on cover slips (Fisher Scientific, USA) previously coated with gelatin (0.1%; Sigma, USA) in a 24-well plate. Ox-LDL (100μg/ml, Sigma, USA), live *C. pneumoniae* (5×10^5 IFU/ml), and GW3965 (1μM), a specific LXR agonist, were added, and 24 hours later Oil red O staining was performed. Quantification of foam cells was calculated using Image-Pro Plus software (Media Cybernetics, Silver Spring, MD) by counting the Oil red O-positive cells and comparing that to the total amount of macrophages (expressed as %foam cells/total macrophages).

GM-CSF Induction by *C. pneumoniae* in Murine Endothelial Cells

Primary murine aortic endothelial cells (ECs) were isolated and purified to over 95% purity from wild type, MyD88$^{-/-}$, TLR2$^{-/-}$, and TLR4$^{-/-}$ mice as we previously described (16,31) ECs were grown to 80% confluency and stimulated overnight with live *C. pneumoniae* (MOI = 5 and MOI = 10). GM-CSF release into the cell-free supernatant was determined after 24 hours of treatment using ELISA (eBioscience, San Diego, CA).

GM-CSF Expression by Atherosclerosis Gene Array

Total RNA from infected and uninfected ApoE−/− mice aorta were isolated using RNeasy mini kit (Qiagen, Valencia, CA) and probed to mouse cardiovascular disease gene array II: Atherosclerosis cDNA gene array following the manufacturer's recommendations (SuperArray Bioscience Corporation, Frederick, MD). Analysis of the images and quantification was performed by the GE Array Expression Analysis Suite (SuperArray Bioscience Corporation) software, and genes of interest were normalized to the housekeeping gene GAPDH.

GM-CSF Expression by Real Time-PCR

Total RNA was isolated from aorta of infected and uninfected ApoE−/− mice by using RNeasy mini kit (Qiagen, Valencia, CA) and subjected to DNase treatment (Invitrogen) to eliminate possible DNA contaminations. cDNA synthesis was performed using Omniscript kit (Qiagen, Valencia, CA). QRT-PCR assays were performed using an iCycler Thermal Cycler (Bio-Rad Laboratories) in 96-well plates using the SYBR Green method (Applied Biosystems, Foster City, CA). Murine GM-CSF primers were as followed: 5′ – GCCATCAAAGAAGCCCTGAA-3′ and 5′-GCGGGTCTGCACACATGTTA-3′ (Applied Biosystems). GAPDH was used as a housekeeping marker. Data were expressed as relative expression of GM-CSF compared to GAPDH.

GM-CSF expression by Immunofluorescence

Cryosections from the aortic sinus of *C. pneumoniae* - infected ApoE−/− mice or uninfected littermate controls were stained for GM-CSF (rat anti-mouse GM-CSF, US Biological). Three to four sections from three to five animals per group were analyzed. Sections were fixed in 1% PFA and dried at room temperature. Sections were then blocked in 5% rabbit serum appropriate for the biotinylated secondary antibody used (rabbit anti-rat, Vector Labs). Staining was detected using the Alkaline Phosphatase Standard ABC Kit (Vector Labs) and Vector Red as a substrate that fluoresces in a spectrum similar to Rhodamine as described earlier (32). Sections were counterstained with DAPI and imaged using a florescent microscope. Omission of the primary antibody and isotype control antibody were included as controls and to determine staining specificity. Quantitative staining for GM-CSF was performed with Image-Pro Plus (Media Cybernetics, Silver Spring, MD). Image analysis was performed by a trained observer blinded to the genotypes of mice as previously described (16). The lesion area and GM-CSF stained areas in the aortic sinus were measured. GM-CSF staining in aortic root plaques was expressed as the percent of positive stained area divided by the total plaque area.

Statistical Analysis

Data are presented as mean values ± SEM. Statistically significant differences were defined as $p < 0.05$ using Student's *t*- test and one-way ANOVA for multiple comparisons.

RESULTS

C. pneumoniae Infection and Serum Cholesterol and Triglyceride Levels

We administered *C. pneumoniae* or an equivalent volume of buffer intranasally to $ApoE^{-/-}$, $ApoE^{-/-}TLR4^{-/-}$, $ApoE^{-/-}TLR2^{-/-}$ $ApoE^{-/-}MyD88^{-/-}$, and $ApoE^{-/-}/LXR\alpha^{-/-}$ mice and control littermates ($ApoE^{-/-}TLR4^{+/+}$, $ApoE^{-/-}TLR2^{+/+}$, $ApoE^{-/-}MyD88^{+/+}$, and $ApoE^{-/-}/LXR\alpha^{+/+}$. Mice were started on a high fat diet (at age 8 weeks) and then infected once a week for 3 consecutive weeks, and high fat diet was maintained until the time of sacrifice 4 months later (Fig. 1A). The dose of *C. pneumoniae* was chosen to ensure that infection was sub-lethal, and was based on estimates of mortality after infection in wild-type and $ApoE^{-/-}$ mice (33). Serum cholesterol and plasma triglyceride concentrations were similar in *C. pneumoniae* infected or uninfected mice (Supplemental Table I). There were also no significant differences in lipoprotein profiles between various genotypes (data not shown).

C. *pneumoniae* Infection Accelerates Atherosclerosis in $ApoE^{-/-}$ Mice

Quantification of the lesion area of aortic sinus plaques revealed a significant increase in lesion size in infected $ApoE^{-/-}$ mice compared to mock-infected littermate controls ($p < 0.01$, Fig. 1B). Infection with *C. pneumoniae* also significantly increased the extent of lipid accumulation in both the aortic sinus plaque lesions ($p < 0.01$; 153 % average increase; Fig. 1B, C) and the total lesion area in the *en face* aorta ($p < 0.01$; 122% average increase; Fig. 1D–E). All infected mice developed similar levels of specific Ab titers against *C. pneumoniae*, while all uninfected controls were antibody negative (data not shown).

TLR2, TLR4 and MyD88 are Required for *C. pneumoniae*-Induced Acceleration of Atherosclerosis

We generated double knockout mice by crossing $ApoE^{-/-}$ mice with either $TLR2^{-/-}$, $TLR4^{-/-}$, or $MyD88^{-/-}$ mice (16). Mice from all genotypes were backcrossed against the C57BL/6 strain for at least 8 generations to enhance congenicity and reduce secondary sources of variance. Littermates that were $ApoE^{-/-}$ but wild-type for TLR2, TLR4, or MyD88 served as controls. Consistent with previous reports by us and others (16,17), uninfected $ApoE^{-/-}TLR2^{-/-}$, $ApoE^{-/-}TLR4^{-/-}$, and $ApoE^{-/-}MyD88^{-/-}$ mice demonstrated a reduction

in cross sectional area of the lesion, lipid content in aortic sinus plaques and a reduction in the size of atherosclerotic lesions in the aorta compared to littermate controls (Fig. 2A, B, C). However, following *C. pneumoniae* infection, cross sectional lesion area and plaque lipid content in aortic sinuses (expressed as percentage of plaque area; Fig. 2A, B) and aortic lesion size (Fig. 2C) were significantly reduced in ApoE$^{-/-}$TLR2$^{-/-}$, ApoE$^{-/-}$TLR4$^{-/-}$ and ApoE$^{-/-}$MyD88$^{-/-}$ mice compared to infected ApoE$^{-/-}$ littermate controls (Fig. 2A, B, C). These reductions in lesion areas in the aortic sinus plaques averaged approximately 60%, 70% and 70% in ApoE$^{-/-}$TLR2$^{-/-}$, ApoE$^{-/-}$TLR4$^{-/-}$ and ApoE$^{-/-}$MyD88$^{-/-}$ infected mice respectively (Fig. 2B). Aorta lesion sizes (en face) were reduced by approximately 70%, 45% and 65% in ApoE$^{-/-}$TLR2$^{-/-}$, ApoE$^{-/-}$TLR4$^{-/-}$ and ApoE$^{-/-}$MyD88$^{-/-}$ infected mice, respectively (Fig. 2C, 2D). Hence, while *C. pneumoniae* infection induced an average of 153% increase in aortic plaque lipid content and 122% increase in aortic lesion size in ApoE$^{-/-}$ mice, it failed to induce a significant acceleration of atherosclerosis in the ApoE$^{-/-}$TLR2$^{-/-}$, ApoE$^{-/-}$TLR4$^{-/-}$ and ApoE$^{-/-}$MyD88$^{-/-}$ double knockout mice despite a modest stimulatory effect (Fig. 2A–C) (specific p values are provided in Supplemental Table II). Furthermore, the significantly reduced acceleration of *C. pneumoniae*-induced atherosclerotic lesions in ApoE$^{-/-}$MyD88$^{-/-}$ mice was not due to reduced bacterial infectivity in MyD88-deficient macrophages. Indeed, if anything MyD88$^{-/-}$ mice have diminished bacterial lung clearance of *C. pneumoniae* (33) and ApoE$^{-/-}$MyD88$^{-/-}$ macrophages have higher level of infectivity compared to ApoE$^{-/-}$ macrophages in-vitro (Data not shown).

Infection-induced Acceleration of Atherosclerosis in ApoE$^{-/-}$ Mice is Associated with Increased Circulating Levels of Inflammatory Cytokines

C. pneumoniae infection in ApoE$^{-/-}$ mice was associated with significant increases in serum concentrations of MCP-1 (Fig. 3A), IL-12p40 (Fig. 3B), TNF-α (Fig. 3C) and IL-6 (Fig. 3D). In contrast, *C. pneumoniae* infection did not increase circulating concentrations of these cytokines in ApoE$^{-/-}$ mice lacking either TLR2, TLR4, or MyD88 (Fig. 4A, 4B and data not shown). These results appear most consistent with the interpretation that at least part of the acceleration of atherosclerosis observed in *C. pneumoniae*-infected ApoE$^{-/-}$ mice may be mediated by a general increase in circulating levels of pro-atherogenic inflammatory cytokines. Circulating IL-12p40 was significantly reduced in uninfected ApoE$^{-/-}$MyD88$^{-/-}$ mice compared to ApoE$^{-/-}$ mice (Fig. 4A), as we have previously reported (16).

Infection-induced Acceleration of Atherosclerosis is Associated with Increased Numbers of Activated Dendritic Cells in Aortic Sinus Plaques

DCs directly control immune responses that occur during inflammatory diseases such as atherosclerosis (34–36). DCs are present in normal arteries, but the numbers of activated DCs increases as atherosclerosis develops (26,37–39). We reasoned that after infection of atherosclerosis-prone mice with *C. pneumoniae*, activated DC numbers in the aortic sinus plaques should increase, but this response should be blunted in mice genetically deficient in TLR2, TLR4, or MyD88. To test this, we performed immunohistochemical staining using MIDC-8 Ab to quantitatively measure numbers of mature, activated myeloid DCs as reported by several investigators (27–30). As anticipated, infection of ApoE$^{-/-}$ mice with *C. pneumoniae* led to a significant increase in the numbers of activated, mature DCs in the aortic sinus plaques ($p < 0.0005$, Fig. 5A, B). In contrast, *C. pneumoniae* infected ApoE$^{-/-}$TLR2$^{-/-}$, ApoE$^{-/-}$TLR4$^{-/-}$ and ApoE$^{-/-}$MyD88$^{-/-}$ mice showed no such increase following infection, and also had significantly lower numbers of activated DCs in the aortic sinus plaques compared to infected ApoE$^{-/-}$ mice ($p< 0.0001$, Fig. 5A, B). MIDC-8 positive DCs were also CD11c + by immunohistochemistry in sequentially obtained slides (data not shown). The striking differences in DC numbers seen between genotypes were not due to an overall reduction in cellularity in the double knockout mice as the cellularity was comparable between genotypes (data not shown). These data suggest that acceleration of atherosclerosis

induced by *C. pneumoniae* infection is accompanied by increased numbers of activated DCs in plaques, but as was the case with lesion size and circulating cytokine levels, this was significantly blocked in ApoE$^{-/-}$ mice with additional genetic deficiencies in TLR2, TLR4 or MyD88.

Shaposhnik et al. (32) recently reported that lack of GM-CSF in hypercholesterolemic mice resulted in smaller lesions and a dramatic decrease in the numbers of DCs in plaques. We therefore reasoned that *C. pneumoniae* infection could stimulate expression of GM-CSF, which in turn might lead to increased recruitment of DCs to plaques and/or increased retention within plaques. To address this possibility, we isolated primary mouse aortic endothelial cells (MAECs) from wild type or TLR2, TLR4 or MyD88 knockout mice, treated the cells with *C. pneumoniae* (or buffer), and assessed GM-CSF secretion. As anticipated, infection of MAEC with *C. pneumoniae* (MOI of 5 and 10) significantly increased GM-CSF release, whereas the genetic absence of TLR2, TLR4 and MyD88 completely abolished the release of the growth factor (Fig. 6A). These results suggest the differential induction of *C. pneumoniae*-induced GM-CSF production may play a role in the significantly increased accumulation of activated DCs in the aortic sinus plaques that we observed following infection in ApoE$^{-/-}$ mice but not in ApoE$^{-/-}$TLR2$^{-/-}$, ApoE$^{-/-}$TLR4$^{-/-}$ and ApoE$^{-/-}$MyD88$^{-/-}$ mice (Fig. 5). Consistent with this interpretation, we also observed significantly increased GM-CSF gene expression in the aorta of ApoE$^{-/-}$ mice infected with *C. pneumoniae* when compared to uninfected littermate control ApoE$^{-/-}$ mice. The Gene Array showed 2.5-fold increase expression of GM-CSF in the aorta of infected mice compared to uninfected controls (data not shown). This observation was confirmed by quantitative real time PCR assay that showed significantly increased GM-CSF expression in infected mice (Fig. 6B). Furthermore, GM-CSF protein was expressed more prominently in the aortic sinus lesions in infected versus uninfected ApoE$^{-/-}$ mice by immunohistochemistry (Fig. 6C).

LXRα Deficiency is Associated with further Acceleration of *C. pneumoniae*-mediated Increase of Atherosclerotic Lesions in ApoE$^{-/-}$Mice

LXRs orchestrate whole-body cholesterol homeostasis, especially macrophage cholesterol metabolism and apoptosis (25). However, LXR activation is negatively influenced by TLR-dependent signaling, and in turn LXRα suppresses expression of downstream targets of TLR signaling (23). These crosstalk mechanisms can importantly modulate atherogenesis; hence, mice with genetic deficiency in both LXRα and ApoE develop accelerated atherosclerosis (40), and this can be reversed by administration of LXR agonists (41). We therefore hypothesized that LXRα and TLR/MyD88 signaling pathways would show reciprocal modulation of *C. pneumoniae*–induced acceleration of atherosclerosis in ApoE$^{-/-}$ mice. If so, then ApoE$^{-/-}$/LXRα$^{-/-}$ double knockout mice should be particularly susceptible to *C. pneumoniae*-induced acceleration of atherosclerosis. As expected, uninfected ApoE$^{-/-}$LXRα$^{-/-}$ compound mutant mice developed increased atherosclerotic lesions in both *en face* aorta and aortic sinus lesions and increased lipid accumulation in the aortic sinus plaques compared to uninfected ApoE$^{-/-}$LXRα$^{+/+}$ littermates (Figs. 7A, B, C). Infection with *C. pneumoniae* markedly enhanced aortic sinus lesion area (80% increase, Fig. 7A), and also resulted in a significantly greater accumulation of lipid in lesions in the aortic sinus and in the aorta en face (Figs. 7B, C). Infection with *C. pneumoniae* significantly increased serum levels of IL-6 and TNF-α as well (Figs. 4C, D). This could not be explained by differing levels of serum cholesterol, since serum cholesterol levels in ApoE$^{-/-}$LXRα$^{-/-}$ and ApoE$^{-/-}$LXRα$^{+/+}$ were similar, regardless of whether mice were infected or not (Supplemental Table I). Furthermore, *C. pneumoniae*-induced acceleration of atherosclerotic plaques in ApoE$^{-/-}$LXRα$^{-/-}$ mice was not due to increased bacterial infectivity in macrophages or degree of lung infectivity or delayed bacterial lung clearance in ApoE$^{-/-}$LXRα$^{-/-}$ compared to ApoE$^{-/-}$ mice (Data not shown).

LXR Signaling Significantly Reduces *C. pneumoniae*-Induced Foam Cell Formation *In Vitro*

The results in the previous section are consistent with the notion that lack of LXRα facilitated acceleration of atherosclerosis by removing inhibitory constraints against TLR-mediated signaling instigated by *C. pneumoniae*. However, LXR-dependent signaling also induces reverse cholesterol transport by macrophages. We therefore reasoned that LXR agonists might suppress *C. pneumoniae*-induced foam cell formation in macrophages *in vitro*. To further evaluate this possibility, we isolated peritoneal-derived macrophages from wild type C57BL/6 mice and stimulated them with oxidized LDL (ox-LDL) and live *C. pneumoniae*. As anticipated, treatment of macrophages with ox-LDL (100 μg/ml) and live *C. pneumoniae* (5×10^5 IFU/ml) induced a significant increase in formation of foam cells ($p < 0.0001$; Figs. 8A, B). However, co-treatment with the LXR agonist GW3965 (1 μM) together with ox-LDL and live *C. pneumoniae* significantly decreased foam cell formation (Figs. 8A, B). Similar results were obtained when cells were co-treated with ox-LDL, GW3965, and UV-killed *C. pneumoniae* (data not shown). These findings suggest that LXR signaling may counter acceleration of atherogenesis and foam cell formation both by promoting cholesterol efflux and by blocking TLR-dependent stimulation of pro-inflammatory signaling.

DISCUSSION

Although numerous epidemiologic (42–44) and experimental (7,9,10) studies link infection with development of atherosclerosis and cardiovascular outcomes, the precise mechanisms contributing to this link have remained elusive. Here we report data that provide new insight into molecular pathways linking *C. pneumoniae* infection to accelerated atherosclerosis in murine models. Consistent with previous studies (7,9,10), we found that infection of atherosclerosis-prone hypercholesterolemic $ApoE^{-/-}$ mice with *C. pneumonia* resulted in accelerated atherosclerosis associated with increased plaque lipid content, numbers of activated DCs in lesions, and serum levels of pro-inflammatory cytokines (IL-12p40, MCP-1, TNF-α and IL-6) compared to mock-infected littermate controls. Conversely, in $ApoE^{-/-}$ mice with additional genetic deficiency in either TLR2, TLR4, or the common adaptor MyD88, atherosclerotic plaque development was significantly inhibited, and this was accompanied by significant reductions in lesion lipid content, numbers of activated DCs in lesions, and serum levels of pro-inflammatory cytokines.

It is important to note that not all pathogens seem to be capable of promoting atherogenesis. Atherosclerotic lesions in mice did not develop after infection with *Chlamydia trachomatis* (45). Furthermore, the atypical bacterial pathogen *Mycoplasma pneumoniae*, which causes lung pathology similar to *C. pneumoniae*, failed to cause inflammatory changes or induce atherosclerotic lesions in rabbits (46). On the other hand, *C. pneumoniae*-induced acceleration of atherosclerosis require viable organism replication (47). Other studies using alternative modes of delivery such as local carotid artery application or intravenous injection also indicate that infection with the live bacteria is necessary to promote plaque development (8). Collectively, these data suggest that either pre-existing heat labile factors, organism replication, or perhaps more likely, continued chronic infection and inflammation was essential for *C. pneumoniae*-induced acceleration of atherosclerosis.

Several investigators proposed that the extent of infectious burden from all pathogenic sources is the key determinant of the impact of pathogens on the atherosclerotic disease process (48–51). Our data suggest a reason why this may be so. Molecular motifs derived from *C. pneumoniae* are detected by multiple TLRs (52–55). In our study, we clearly show that either TLR2 or TLR4 can mediate the pro-atherogenic effects of *C. pneumoniae* infection. While the $ApoE^{-/-}/TLR2^{-/-}$, $ApoE^{-/-}/TLR4^{-/-}$ and $ApoE^{-/-}/MyD88^{-/-}$ double knockout mice displayed a substantially reduced pro-atherogenic response to infection, the modest 17–30% increases in lesion size we noted are consistent with the interpretation that TLR-independent

signaling and/or MyD88-independent signaling may also contribute to some extent to infection-mediated progression of atherosclerosis. Together, these data strongly suggest that *C. pneumoniae* can exacerbate atherosclerosis in multiple ways that involve innate immune signaling networks.

Recent studies indicate an important role of DCs in atherosclerosis (38). We observed that *C. pneumoniae*-induced acceleration of atherosclerosis was similarly accompanied by significantly increased numbers of activated DCs accumulating in plaques from infected ApoE-null mice when compared to uninfected littermate controls. No such increase in DC numbers was observed in infected ApoE$^{-/-}$TLR2$^{-/-}$, ApoE$^{-/-}$TLR4$^{-/-}$ and ApoE$^{-/-}$MyD88$^{-/-}$ mice. Of interest, Shaposhnik et al. showed that GM-CSF plays a key role in DC migration into lesions, and that LDLR$^{-/-}$ GM-CSF$^{-/-}$ mice exhibit both diminished lesion size and decreased DC accumulation in the plaques (32). Accordingly, we observed that *C. pneumoniae* induces a dose-dependent release of GM-CSF in primary aortic endothelial cells (EC) in a TLR2-, TLR4-, and MyD88-dependent manner. We also observed that GM-CSF gene expression was significantly higher in the aortic tissue as well as aortic sinus lesions obtained from infected ApoE$^{-/-}$ mice compared to uninfected littermate controls. Therefore, it is tempting to propose that the differential GM-CSF induction by *C. pneumoniae* observed in wild type ECs *versus* TLR2$^{-/-}$, TLR4$^{-/-}$, or MyD88$^{-/-}$ ECs may play a role in recruiting and/or retaining DCs into developing plaques, and may provide an additional explanation for how *C. pneumoniae* accelerates plaque formation. While we used an EC infection model for these studies to show that *C. pneumoniae* can induce GM-CSF in-vitro, the mechanism of GM-CSF induction during in-vivo infection may be different and may be indirectly modulated by the induced cytokines.

Our data also provide important new evidence that suggests that LXR activation integrates cholesterol homeostasis with innate immune host defences in a manner that can critically modulate atherogenesis. When mice with genetic deficiency of both ApoE and LXRα were challenged with *C. pneumoniae*, markedly accelerated atherosclerosis occurred that was significantly greater than that observed in either ApoE$^{-/-}$LXRα$^{+/+}$ littermate controls or uninfected ApoE$^{-/-}$LXRα$^{-/-}$ controls. *In vitro* studies with peritoneal-derived cells obtained from wild type mice showed that treatment with GW3965, an LXR agonist, inhibited foam cell formation induced by ox-LDL and live C. *pneumoniae.* Collectively then, our data indicate that 1) *C. pneumoniae* infection does indeed accelerate atherogenesis in hypercholesterolemic mice in a TLR/MyD88-dependent manner, perhaps in part through a significant increase in serum cytokine levels and accumulation of activated DCs in the aortic sinus lesions; and 2) pro-atherogenic effects of *C. pneumoniae* infection are substantially enhanced with genetic deficiency of LXRα.

Previous reports indicate that signaling triggered by TLR3 or TLR4 can inhibit expression of LXR target genes (23). On the other hand, *C. pneumoniae* promotes foam cell formation in a TLR2-dependent manner, but this can be counteracted by treatment with LXR agonists (52). Gain and loss of function studies both indicate that LXRα activation retards atherogenesis by promoting cholesterol efflux (40). The model that emerges suggests that TLR-dependent signaling and LXR activity reciprocally modulate one another. Our results extend this theme, and show that when this balance is tipped by *C. pneumoniae*-induced innate immune signaling, acceleration of atherosclerosis occurs. Acceleration of atherosclerosis in LXR-deficient mice cannot be attributed to compromised host immune defenses, since *in vitro* infectivity of ApoE$^{-/-}$/LXRα$^{-/-}$ and ApoE$^{-/-}$/LXRα$^{+/+}$ macrophages with *C. pneumoniae* was similar (data not shown). Instead, acceleration of atherosclerosis in ApoE$^{-/-}$/LXRα$^{-/-}$ mice was probably due at least in part to defective cholesterol efflux by macrophages. Hence, our data suggest that infection in the setting of hypercholesterolemia and lack of LXRα signaling promotes atherogenesis most likely by two mechanisms: defective reverse cholesterol transport and inflammation instigated by *C. pneumonia* that in turn triggers TLR-dependent signaling.

We demonstrate here that *C. pneumoniae* can directly influence atherosclerotic plaque development in TLR2-, TLR4-, and MyD88-dependent manner by promoting foam cell formation and enhancing recruitment and/or retention of activated DCs in plaques. On the other hand, LXR signaling may counteract *C. pneumoniae*-induced atherosclerosis in at least two ways: by decreasing foam cell formation by promoting cholesterol efflux, and by blocking TLR-dependent stimulation of pro-inflammatory signaling. Our data thus suggest a close interaction between cholesterol homeostatic pathways orchestrated by LXRs and innate immune host defenses such as TLRs. This reciprocal relationship may become skewed in favour of inflammation (and hence accelerated atherosclerosis) when infection with *C. pneumoniae* occurs, at least in the setting of hypercholesterolemia. Whether other pathogens that have been linked to atherosclerosis might similarly alter this balance will be an intriguing question to be addressed by future studies.

Acknowledgements

This work was supported by grants from the NIAID and HNLBI (5R01AI058128, 5R01AI067995, and RO1HL66436 to MA), and NHLBI (2P01HL030568 and 5R01HL066088 to PT). P. Tontonoz is an investigator of the Howard Hughes Medical Institute.

ABBREVIATIONS

C.pn
: *Chlamydia pneumoniae*

DC
: dendritic cell

EC
: endothelial cell

TLR
: Toll-like receptor

MyD88
: Myeloid Differentiation factor 88

LXR
: liver X Receptor

ox-LDL
: oxidized low-density lipoprotein

ApoE
: apolipoprotein E

References

1. Ezzahiri R, Stassen FR, Kurvers HR, Dolmans V, Kitslaar PJ, Bruggeman CA. Chlamydia pneumoniae infections augment atherosclerotic lesion formation: a role for serum amyloid P. Apmis 2006;114:117–126. [PubMed: 16519748]
2. Saikku P, Leinonen M, Mattila K, Ekman MR, Nieminen MS, Makela PH, Huttunen JK, Valtonen V. Serological evidence of an association of a novel Chlamydia, TWAR, with chronic coronary heart disease and acute myocardial infarction. Lancet 1988;2:983–986. [PubMed: 2902492]
3. Kuo CC, Gown AM, Benditt EP, Grayston JT. Detection of Chlamydia pneumoniae in aortic lesions of atherosclerosis by immunocytochemical stain. Arterioscler Thromb 1993;13:1501–1504. [PubMed: 7691166]

4. Grayston JT, Kuo CC, Coulson AS, Campbell LA, Lawrence RD, Lee MJ, Strandness ED, Wang SP. Chlamydia pneumoniae (TWAR) in atherosclerosis of the carotid artery. Circulation 1995;92:3397–3400. [PubMed: 8521559]
5. Kuo CC, Coulson AS, Campbell LA, Cappuccio AL, Lawrence RD, Wang SP, Grayston JT. Detection of Chlamydia pneumoniae in atherosclerotic plaques in the walls of arteries of lower extremities from patients undergoing bypass operation for arterial obstruction. J Vasc Surg 1997;26:29–31. [PubMed: 9240318]
6. Tormakangas L, Erkkila L, Korhonen T, Tiirola T, Bloigu A, Saikku P, Leinonen M. Effects of repeated Chlamydia pneumoniae inoculations on aortic lipid accumulation and inflammatory response in C57BL/6J mice. Infect Immun 2005;73:6458–6466. [PubMed: 16177317]
7. Blessing E, Campbell LA, Rosenfeld ME, Chough N, Kuo CC. Chlamydia pneumoniae infection accelerates hyperlipidemia induced atherosclerotic lesion development in C57BL/6J mice. Atherosclerosis 2001;158:13–17. [PubMed: 11500169]
8. Hauer AD, de Vos P, Peterse N, ten Cate H, van Berkel TJ, Stassen FR, Kuiper J. Delivery of Chlamydia pneumoniae to the vessel wall aggravates atherosclerosis in LDLr−/− mice. Cardiovasc Res 2006;69:280–288. [PubMed: 16112098]
9. Moazed TC, Campbell LA, Rosenfeld ME, Grayston JT, Kuo CC. Chlamydia pneumoniae infection accelerates the progression of atherosclerosis in apolipoprotein E-deficient mice. J Infect Dis 1999;180:238–241. [PubMed: 10353889]
10. Rothstein NM, Quinn TC, Madico G, Gaydos CA, Lowenstein CJ. Effect of azithromycin on murine arteriosclerosis exacerbated by Chlamydia pneumoniae. J Infect Dis 2001;183:232–238. [PubMed: 11120929]
11. Aalto-Setala K, Laitinen K, Erkkila L, Leinonen M, Jauhiainen M, Ehnholm C, Tamminen M, Puolakkainen M, Penttila I, Saikku P. Chlamydia pneumoniae does not increase atherosclerosis in the aortic root of apolipoprotein E-deficient mice. Arterioscler Thromb Vasc Biol 2001;21:578–584. [PubMed: 11304476]
12. Caligiuri G, Rottenberg M, Nicoletti A, Wigzell H, Hansson GK. Chlamydia pneumoniae infection does not induce or modify atherosclerosis in mice. Circulation 2001;103:2834–2838. [PubMed: 11401941]
13. Kuo CC, Shor A, Campbell LA, Fukushi H, Patton DL, Grayston JT. Demonstration of Chlamydia pneumoniae in atherosclerotic lesions of coronary arteries. J Infect Dis 1993;167:841–849. [PubMed: 8450249]
14. Rosenfeld ME, Blessing E, Lin TM, Moazed TC, Campbell LA, Kuo C. Chlamydia, inflammation, and atherogenesis. J Infect Dis 2000;181(Suppl 3):S492–497. [PubMed: 10839746]
15. Bjorkbacka H V, Kunjathoor V, Moore KJ, Koehn S, Ordija CM, Lee MA, Means T, Halmen K, Luster AD, Golenbock DT, Freeman MW. Reduced atherosclerosis in MyD88-null mice links elevated serum cholesterol levels to activation of innate immunity signaling pathways. Nat Med 2004;10:416–421. [PubMed: 15034566]
16. Michelsen KS, Wong MH, Shah PK, Zhang W, Yano J, Doherty TM, Akira S, Rajavashisth TB, Arditi M. Lack of Toll-like receptor 4 or myeloid differentiation factor 88 reduces atherosclerosis and alters plaque phenotype in mice deficient in apolipoprotein E. Proc Natl Acad Sci U S A 2004;101:10679–10684. [PubMed: 15249654]
17. Mullick AE, Tobias PS, Curtiss LK. Modulation of atherosclerosis in mice by Toll-like receptor 2. J Clin Invest 2005;115:3149–3156. [PubMed: 16211093]
18. Schoneveld AH, Hoefer I, Sluijter JP, Laman JD, de Kleijn DP, Pasterkamp G. Atherosclerotic lesion development and Toll like receptor 2 and 4 responsiveness. Atherosclerosis. 2007
19. Krull M, Maass M, Suttorp N, Rupp J. Chlamydophila pneumoniae. Mechanisms of target cell infection and activation. Thromb Haemost 2005;94:319–326. [PubMed: 16113821]
20. Hansson GK. Inflammation, atherosclerosis, and coronary artery disease. N Engl J Med 2005;352:1685–1695. [PubMed: 15843671]
21. Hansson GK, Libby P. The immune response in atherosclerosis: a double-edged sword. Nat Rev Immunol 2006;6:508–519. [PubMed: 16778830]
22. Joseph SB, Tontonoz P. LXRs: new therapeutic targets in atherosclerosis? Curr Opin Pharmacol 2003;3:192–197. [PubMed: 12681243]

23. Zelcer N, Tontonoz P. Liver X receptors as integrators of metabolic and inflammatory signaling. J Clin Invest 2006;116:607–614. [PubMed: 16511593]
24. Castrillo A, Joseph SB, Vaidya SA, Haberland M, Fogelman AM, Cheng G, Tontonoz P. Crosstalk between LXR and toll-like receptor signaling mediates bacterial and viral antagonism of cholesterol metabolism. Mol Cell 2003;12:805–816. [PubMed: 14580333]
25. Joseph SB, Bradley MN, Castrillo A, Bruhn KW, Mak PA, Pei L, Hogenesch J, O'Connell MR, Cheng G, Saez E, Miller JF, Tontonoz P. LXR-dependent gene expression is important for macrophage survival and the innate immune response. Cell 2004;119:299–309. [PubMed: 15479645]
26. Yilmaz A, Rowley A, Schulte DJ, Doherty TM, Schroder NW, Fishbein MC, Kalelkar M, Cicha I, Schubert K, Daniel WG, Garlichs CD, Arditi M. Activated myeloid dendritic cells accumulate and co-localize with CD3+ T cells in coronary artery lesions in patients with Kawasaki disease. Exp Mol Pathol 2007;83:93–103. [PubMed: 17335804]
27. Breel M, Mebius RE, Kraal G. Dendritic cells of the mouse recognized by two monoclonal antibodies. Eur J Immunol 1987;17:1555–1559. [PubMed: 3678361]
28. Inaba K, Pack M, Inaba M, Sakuta H, Isdell F, Steinman RM. High levels of a major histocompatibility complex II-self peptide complex on dendritic cells from the T cell areas of lymph nodes. J Exp Med 1997;186:665–672. [PubMed: 9271582]
29. Serafini B, Columba-Cabezas S, Di Rosa F, Aloisi F. Intracerebral recruitment and maturation of dendritic cells in the onset and progression of experimental autoimmune encephalomyelitis. Am J Pathol 2000;157:1991–2002. [PubMed: 11106572]
30. Bobryshev YV, Taksir T, Lord RS, Freeman MW. Evidence that dendritic cells infiltrate atherosclerotic lesions in apolipoprotein E-deficient mice. Histol Histopathol 2001;16:801–808. [PubMed: 11510970]
31. Shuang C, Wong MH, Schulte DJ, Arditi M, Michelsen KS. Differential expression of Toll-like receptor 2 (TLR2) and responses to TLR2 ligands between human and murine vascular endothelial cells. J Endotoxin Res 2007;13:281–296. [PubMed: 17986487]
32. Shaposhnik Z, Wang X, Weinstein M, Bennett BJ, Lusis AJ. Granulocyte macrophage colony-stimulating factor regulates dendritic cell content of atherosclerotic lesions. Arterioscler Thromb Vasc Biol 2007;27:621–627. [PubMed: 17158354]
33. Naiki Y, Michelsen KS, Schroder NW, Alsabeh R, Slepenkin A, Zhang W, Chen S, Wei B, Bulut Y, Wong MH, Peterson EM, Arditi M. MyD88 is pivotal for the early inflammatory response and subsequent bacterial clearance and survival in a mouse model of Chlamydia pneumoniae pneumonia. J Biol Chem 2005;280:29242–29249. [PubMed: 15964841]
34. Lipscomb MF, Masten BJ. Dendritic cells: immune regulators in health and disease. Physiol Rev 2002;82:97–130. [PubMed: 11773610]
35. Steinman RM. Linking innate to adaptive immunity through dendritic cells. Novartis Found Symp 2006;279:101–109. [PubMed: 17278389]discussion 109–113, 216–109
36. Steinman RM. Dendritic cells: versatile controllers of the immune system. Nat Med 2007;13:1155–1159. [PubMed: 17917664]
37. Angeli V, Llodra J, Rong JX, Satoh K, Ishii S, Shimizu T, Fisher EA, Randolph GJ. Dyslipidemia associated with atherosclerotic disease systemically alters dendritic cell mobilization. Immunity 2004;21:561–574. [PubMed: 15485633]
38. Doherty TM, Fisher EA, Arditi M. TLR signaling and trapped vascular dendritic cells in the development of atherosclerosis. Trends Immunol 2006;27:222–227. [PubMed: 16580258]
39. Trogan E, Feig JE, Dogan S, Rothblat GH, Angeli V, Tacke F, Randolph GJ, Fisher EA. Gene expression changes in foam cells and the role of chemokine receptor CCR7 during atherosclerosis regression in ApoE-deficient mice. Proc Natl Acad Sci U S A 2006;103:3781–3786. [PubMed: 16537455]
40. Bradley MN, Hong C, Chen M, Joseph SB, Wilpitz DC, Wang X, Lusis AJ, Collins A, Hseuh WA, Collins JL, Tangirala RK, Tontonoz P. Ligand activation of LXR beta reverses atherosclerosis and cellular cholesterol overload in mice lacking LXR alpha and apoE. J Clin Invest 2007;117:2337–2346. [PubMed: 17657314]
41. Joseph SB, McKilligin E, Pei L, Watson MA, Collins AR, Laffitte BA, Chen M, Noh G, Goodman J, Hagger GN, Tran J, Tippin TK, Wang X, Lusis AJ, Hsueh WA, Law RE, Collins JL, Willson TM,

Tontonoz P. Synthetic LXR ligand inhibits the development of atherosclerosis in mice. Proc Natl Acad Sci U S A 2002;99:7604–7609. [PubMed: 12032330]

42. Kalayoglu MV, Libby P, Byrne GI. Chlamydia pneumoniae as an emerging risk factor in cardiovascular disease. Jama 2002;288:2724–2731. [PubMed: 12460096]
43. Shor A, Phillips JI. Chlamydia pneumoniae and atherosclerosis. Jama 1999;282:2071–2073. [PubMed: 10591391]
44. Smeeth L, Thomas SL, Hall AJ, Hubbard R, Farrington P, Vallance P. Risk of myocardial infarction and stroke after acute infection or vaccination. N Engl J Med 2004;351:2611–2618. [PubMed: 15602021]
45. Blessing E, Nagano S, Campbell LA, Rosenfeld ME, Kuo CC. Effect of Chlamydia trachomatis infection on atherosclerosis in apolipoprotein E-deficient mice. Infect Immun 2000;68:7195–7197. [PubMed: 11083855]
46. Fong IW, Chiu B, Viira E, Fong MW, Jang D, Mahony J. Rabbit model for Chlamydia pneumoniae infection. J Clin Microbiol 1997;35:48–52. [PubMed: 8968879]
47. Sharma J, Niu Y, Ge J, Pierce GN, Zhong G. Heat-inactivated C. pneumoniae organisms are not atherogenic. Mol Cell Biochem 2004;260:147–152. [PubMed: 15228096]
48. Espinola-Klein C, Rupprecht HJ, Blankenberg S, Bickel C, Kopp H, Rippin G, Victor A, Hafner G, Schlumberger W, Meyer J. Impact of infectious burden on extent and long-term prognosis of atherosclerosis. Circulation 2002;105:15–21. [PubMed: 11772870]
49. Espinola-Klein C, Rupprecht HJ, Blankenberg S, Bickel C, Kopp H, Victor A, Hafner G, Prellwitz W, Schlumberger W, Meyer J. Impact of infectious burden on progression of carotid atherosclerosis. Stroke 2002;33:2581–2586. [PubMed: 12411646]
50. Rupprecht HJ, Blankenberg S, Bickel C, Rippin G, Hafner G, Prellwitz W, Schlumberger W, Meyer J. Impact of viral and bacterial infectious burden on long-term prognosis in patients with coronary artery disease. Circulation 2001;104:25–31. [PubMed: 11435333]
51. Schroeder JS. Infectious burden and atherosclerosis. Curr Cardiol Rep 2002;4:259. [PubMed: 12052264]
52. Cao F, Castrillo A, Tontonoz P, Re F, Byrne GI. Chlamydia pneumoniae--induced macrophage foam cell formation is mediated by Toll-like receptor 2. Infect Immun 2007;75:753–759. [PubMed: 17145941]
53. Prebeck S, Kirschning C, Durr S, da Costa C, Donath B, Brand K, Redecke V, Wagner H, Miethke T. Predominant role of toll-like receptor 2 versus 4 in Chlamydia pneumoniae-induced activation of dendritic cells. J Immunol 2001;167:3316–3323. [PubMed: 11544320]
54. Rodriguez N, Wantia N, Fend F, Durr S, Wagner H, Miethke T. Differential involvement of TLR2 and TLR4 in host survival during pulmonary infection with Chlamydia pneumoniae. Eur J Immunol 2006;36:1145–1155. [PubMed: 16609927]
55. Yang X, Coriolan D, Schultz K, Golenbock DT, Beasley D. Toll-like receptor 2 mediates persistent chemokine release by Chlamydia pneumoniae-infected vascular smooth muscle cells. Arterioscler Thromb Vasc Biol 2005;25:2308–2314. [PubMed: 16179594]

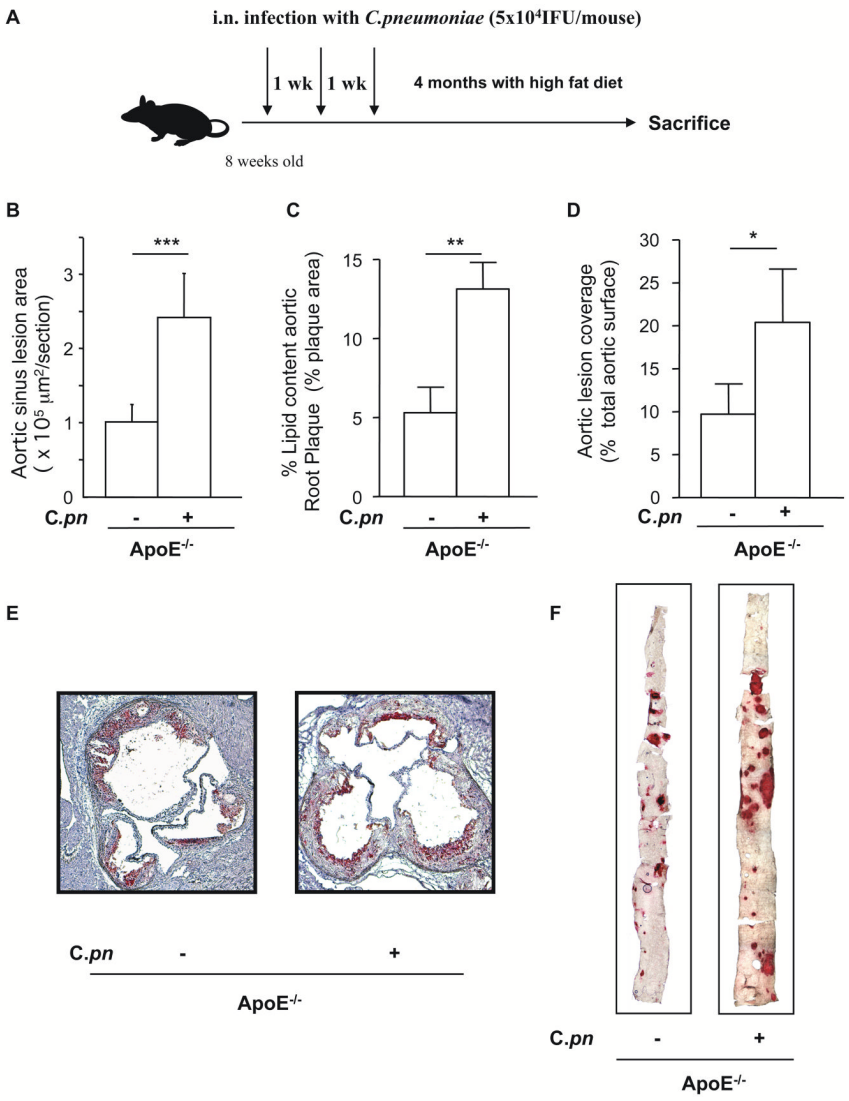

Fig. 1. *C. pneumoniae* infection induces acceleration of atherosclerosis in ApoE$^{-/-}$ mice

ApoE$^{-/-}$ mice were infected intranasally with *C. pneumoniae* (5×10^4 IFU/mouse) three times (one week apart for 3 consecutive weeks), and then fed with a high fat diet for the following 4 months (A). *C. pneumoniae* infection induces acceleration of atherosclerosis as measured by aortic sinus lesion area size (B), increased accumulation of lipid content in the aortic sinus plaques (B-C-E) and *en face* prepared aorta lesion size (D–F) in ApoE$^{-/-}$ mice. Panel E and F are representative experiments showing the accumulation of lipids in the aortic sinus (E) and aorta (F) of C. *pneumoniae*-infected ApoE$^{-/-}$ mice. Oil red O staining was performed and data was expressed as aortic sinus total lesion area or as percentage of lipid content relative to the total area in the aortic sinus to show plaque composition. Aorta lesions were expressed as aortic lesion coverage calculated as percentage of positive areas compared with the total aortic surface (n=12 for the aortic sinus experiments, and n=13 for the *en face* aorta experiments).

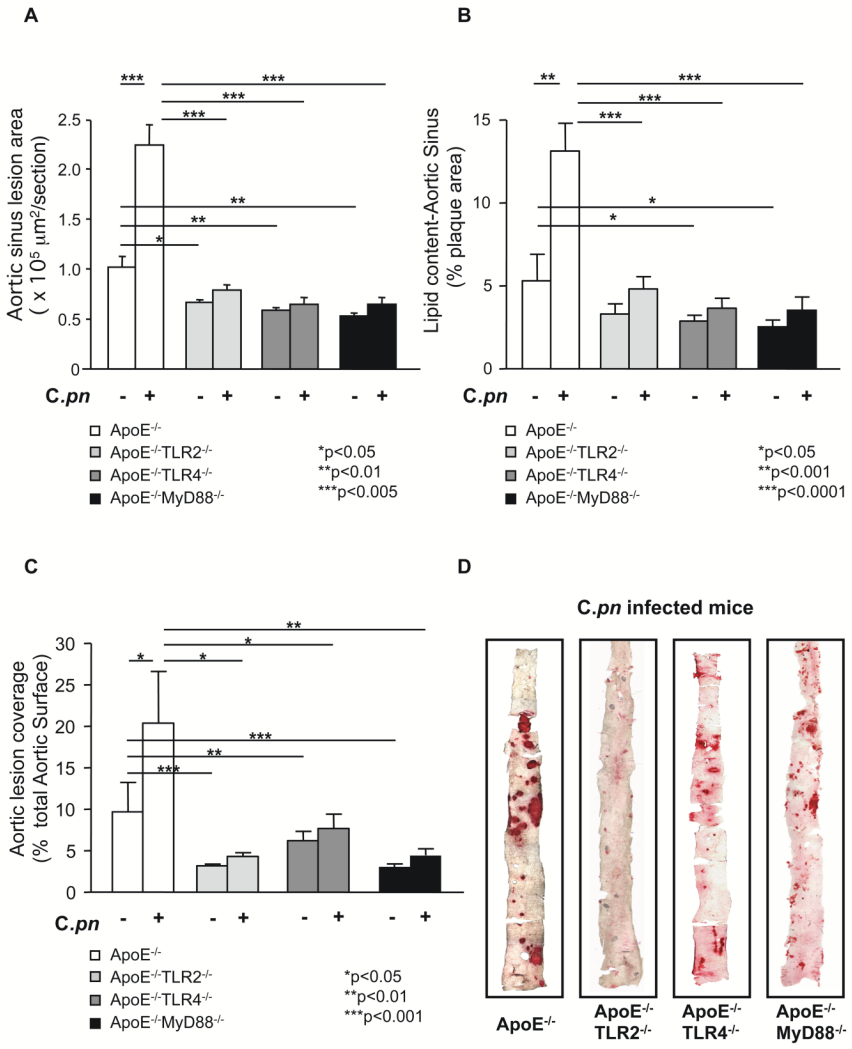

Fig. 2.

C. pneumoniae infection fails to induce acceleration of atherosclerosis in ApoE/TLR2, ApoE/TLR4 and ApoE/MyD88 double knockout mice. Quantification of lipid content in the aortic sinus (A) and aorta lesions en face (C) from ApoE$^{-/-}$TLR2$^{-/-}$, ApoE$^{-/-}$TLR4$^{-/-}$ and ApoE$^{-/-}$MyD88$^{-/-}$ with and without infection. Representative Oil red O staining of aortic sinus (B) and aorta *en face* lesions (D) from infected ApoE$^{-/-}$, ApoE$^{-/-}$TLR2$^{-/-}$, ApoE$^{-/-}$TLR4$^{-/-}$ and ApoE$^{-/-}$MyD88$^{-/-}$ mice are shown. Data are presented as mean values ± SEM, n = 10–12 for the aortic sinus experiments, and n= 10–14 for the *en face* aorta experiments.

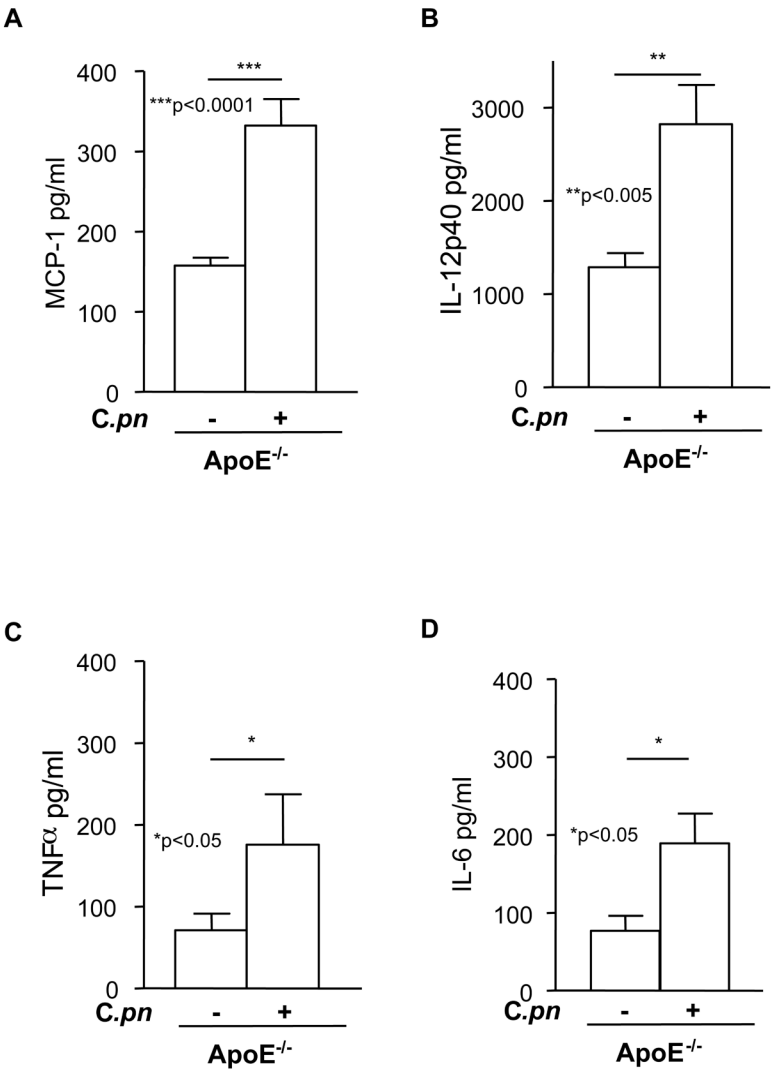

Fig. 3. *C. pneumoniae* infected ApoE$^{-/-}$ mice manifest higher circulating concentrations of cytokines

C. pneumoniae infection increased circulating levels of MCP-1 (A), IL-12p40 (B), TNFα (C) and IL-6 (D) in ApoE$^{-/-}$ mice. Cytokine levels were measured from serum obtained at the time of sacrifice using ELISA. Data are presented as mean values ± SEM (n = 10–12).

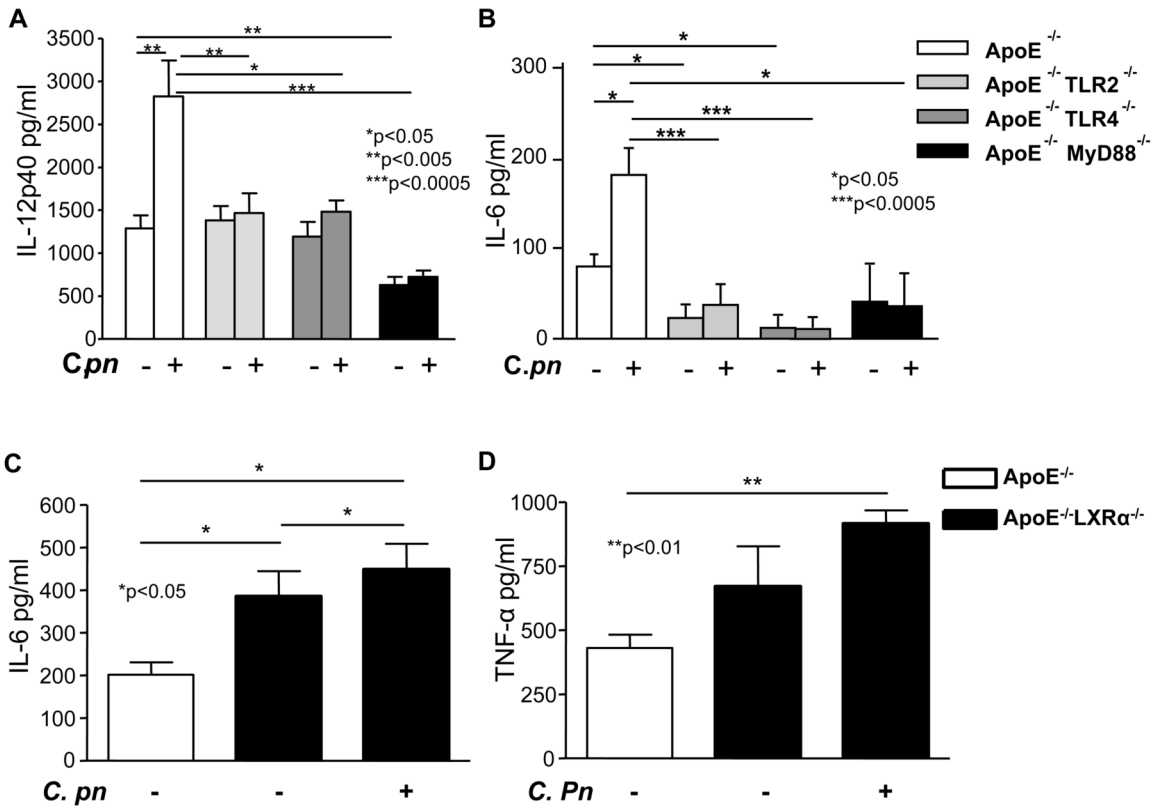

Fig. 4. *C. pneumoniae*-induced acceleration of atherosclerosis in ApoE$^{-/-}$ and in ApoE$^{-/-}$/LXRα$^{-/-}$ mice is associated with increased circulating levels of cytokines

Panels A–B: Infected ApoE-null mice had significantly increased cytokine levels compared to uninfected littermate controls. In contrast, the genetic absence of TLR2, TLR4 and MyD88 significantly reduced serum IL-12p40 (A) and IL-6 (B) in both uninfected and infected ApoE$^{-/-}$ mice. Cytokine concentrations were measured using ELISA. Data are presented as mean values ± SEM, n = 9.

Panels C–D: The genetic absence of LXRα promoted higher circulating levels of IL-6 (C) and TNF-α (D) in uninfected and infected ApoE$^{-/-}$ mice. Data are presented as mean values ± SEM, n = 8–10.

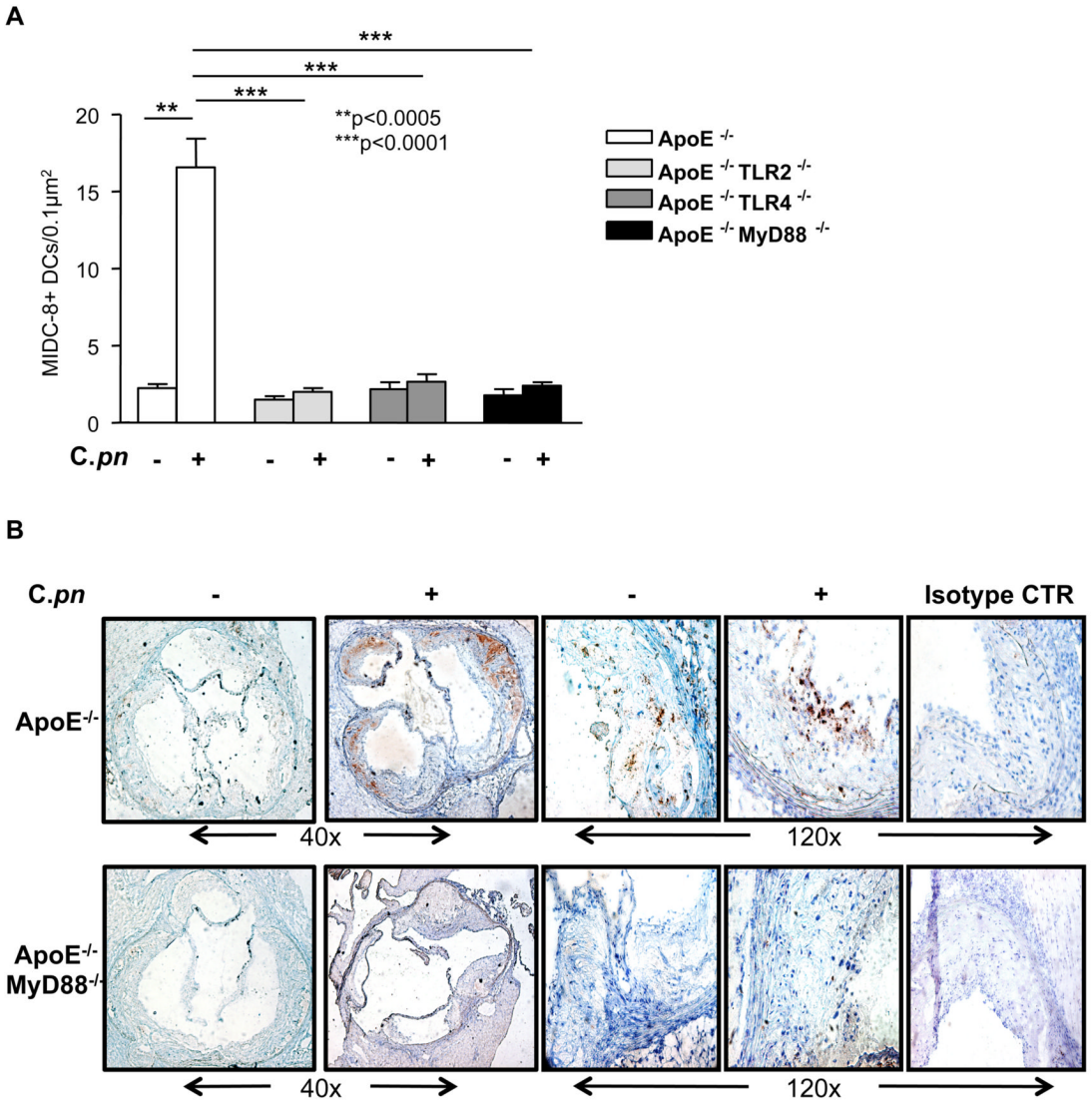

Fig. 5. *C. pneumoniae* infection leads to increased numbers of active DCs in the aortic sinus of ApoE$^{-/-}$ mice

(**Panel A**): Quantification of active DCs in the aortic sinus of infected and non-infected ApoE$^{-/-}$, ApoE$^{-/-}$TLR2$^{-/-}$, ApoE$^{-/-}$TLR4$^{-/-}$ and ApoE$^{-/-}$MyD88$^{-/-}$ mice. (**Panel B**): Representative MIDC-8 positive staining in infected *versus* uninfected ApoE$^{-/-}$ and ApoE$^{-/-}$MyD88$^{-/-}$ mice. Infection with *C. pneumoniae* (5×10^4 IFU/mouse) led to greater accumulation of MIDC-8 positive DCs in the aortic sinus from ApoE$^{-/-}$ mice, but not in ApoE$^{-/-}$TLR2$^{-/-}$, ApoE$^{-/-}$TLR4$^{-/-}$ or ApoE$^{-/-}$MyD88$^{-/-}$ mice. Data are presented mean values ± SEM, n= 10–12.

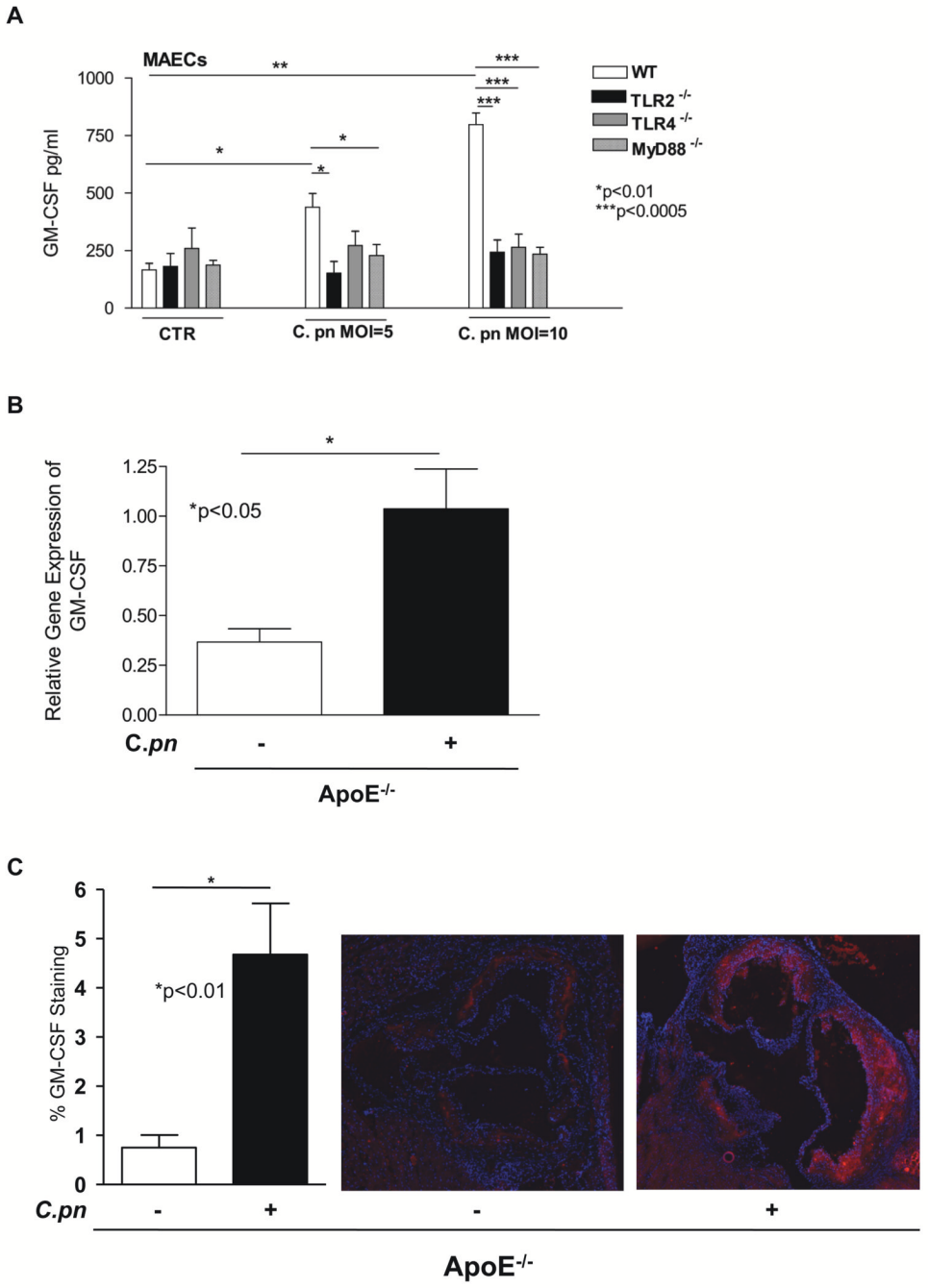

Fig. 6. *C. pneumoniae* induces GM-CSF gene and protein expression in-vitro and in-vivo. Panel A: *C. pneumoniae induces GM-CSF release from primary mouse aortic ECs in a TLR2-, TLR4- and MyD88-dependent manner*

Live *C. pneumoniae* (MOI = 5 and MOI = 10) induced a dose-dependent release of GM-CSF from primary wild-type ECs. On the other hand, the same infection resulted in significantly diminished release of GM-CSF from ECs isolated from TLR2$^{-/-}$, TLR4$^{-/-}$, and MyD88$^{-/-}$ mice. Data are presented as mean values ± SEM, n = 5–7. Statistically significant differences are denoted by *, **, and ***, which indicate $p < 0.05$, $p < 0.01$, and $p < 0.0005$ (Student's t test and one-way ANOVA).

Panel B: ***GM-CSF gene expression was significantly increased in aorta obtained from C. pneumoniae-infected ApoE$^{-/-}$ mice compared to uninfected control mice.*** Comparison of the relative gene expression of GM-CSF was determined by quantitative real-time PCR analyses. The relative expression of GM-CSF in the aortic tissue was assessed in both infected ApoE$^{-/-}$ mice and uninfected littermate ApoE$^{-/-}$ controls. Data were normalized to GAPDH expression (n= 5/group). Values are shown as mean and SEM as relative expression.

Panel C: ***GM-CSF protein expression was increased in the aortic sinus lesions in C. pneumoniae-infected ApoE$^{-/-}$ mice compared to uninfected control mice.*** Sequential aortic sinus sections were used and GM-CSF staining was detected by using the Alkaline Phosphatase Standard ABC Kit and Vector Red as a substrate that fluoresces in a spectrum similar to Rhodamine. Sections were counterstained with DAPI and imaged using a fluorescent microscope. Quantitative measurement of GM-CSF expression was calculated using Image Pro Plus software and expressed as GM-CSF staining area as percent of total aortic sinus lesion area (n= 5/group). Data are presented as mean ± SEM. A representative finding in the aortic sinus lesions among the infected, and uninfected ApoE$^{-/-}$ mice is shown.

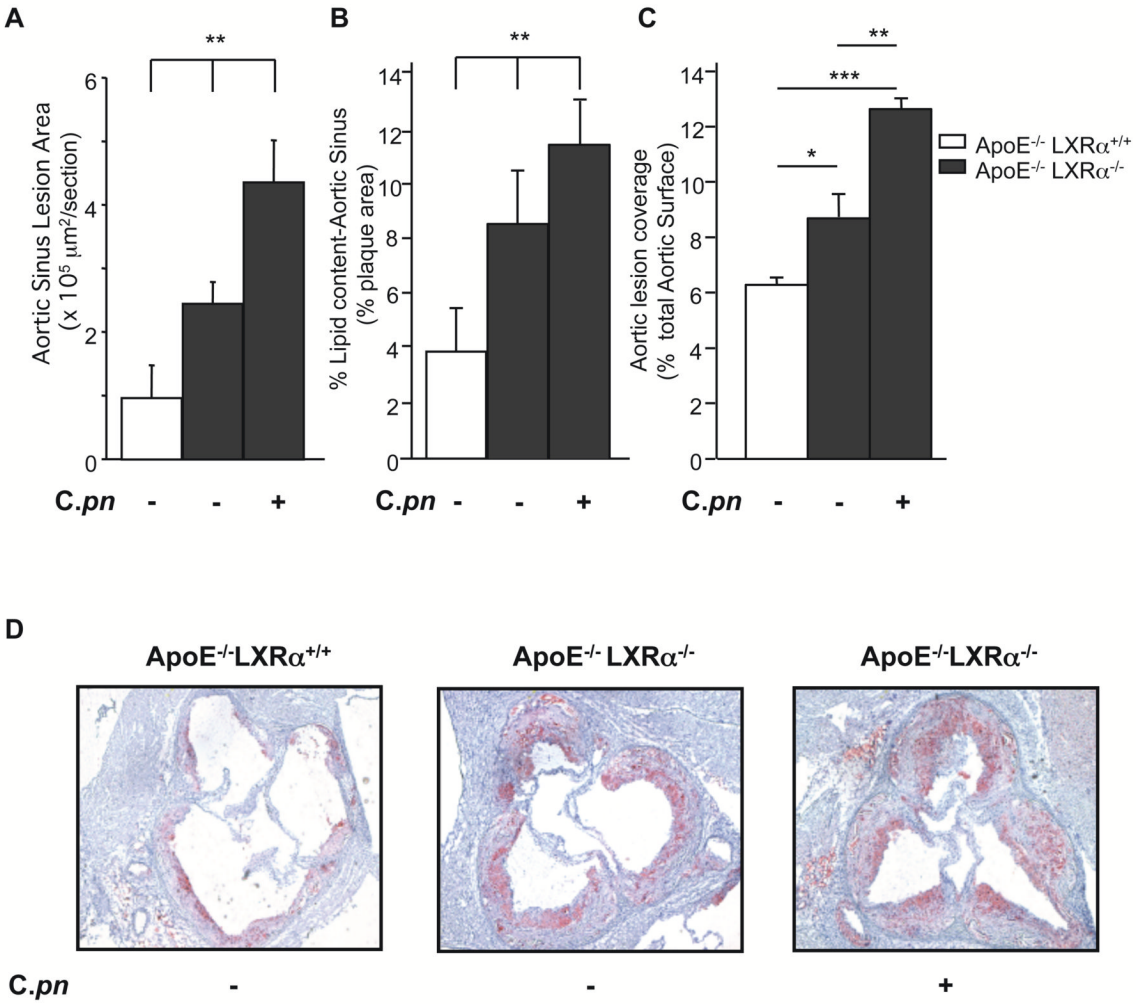

Fig. 7. LXRα deficiency enhances *C. pneumoniae*-mediated acceleration of atherosclerosis in ApoE$^{-/-}$ Mice

Quantification of lesion size shown as area (**A**), and plaque composition as lipid content in the aortic sinus (**B**), and lipid content in aorta lesions en face (**C**) from ApoE$^{-/-}$ LXRα$^{+/+}$ and ApoE$^{-/-}$LXRα$^{-/-}$ with and without *C. pneumoniae* infection (5×10^4 IFU/mouse). (**D**) Representative Oil red O staining of aortic sinus plaques from ApoE$^{-/-}$LXRα$^{+/+}$ and ApoE$^{-/-}$ LXRα$^{-/-}$ mice with and without infection. Lesions from ApoE$^{-/-}$LXRα$^{-/-}$ mice showed increased lipid content after *C. pneumoniae* infection. Data are presented as mean values ± SEM, n= 8–10. Statistically significant differences are denoted by *, **, and ***, which indicate $p < 0.05$, $p < 0.01$ and $p < 0.001$ respectively.

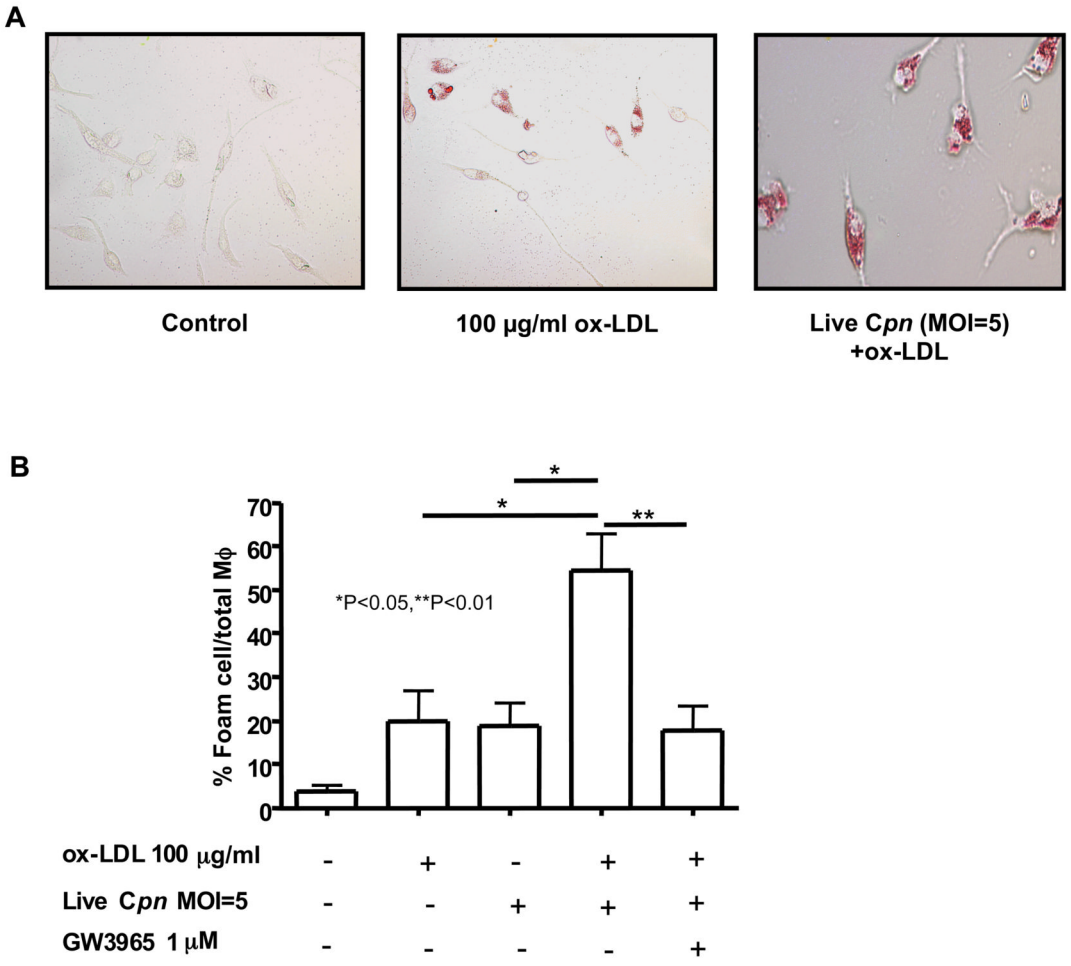

Fig. 8. GW3965, an LXR agonist, reduces ox-LDL and *C. pneumoniae*–induced foam cell formation by peritoneal macrophages

Live *C. pneumoniae* (5×10^5 IFU/ml) induced foam cell formation in the presence ox-LDL (100 µg/ml) in wild-type primary peritoneal macrophages. Representative Oil red O staining of peritoneal macrophage-derived foam cells (A). Treatment of macrophages with GW3965 (1µM), an LXR agonist, reduced foam cells produced after stimulation with *C. pneumoniae* plus ox-LDL (B). Oil red O positive cells were compared with the total amount of macrophages and expressed as % foam cells/total macrophages. Data are presented as mean values ± SEM, n=4.